Preprints of the 19th World Congress
The International Federation of Automatic Control
Cape Town, South Africa. August 24-29, 2014

Robust Sensor Fault-Tolerant Control Scheme for Wind Turbines with Hydrostatic Transmission

Horst Schulte * **Sören Georg** * **Abdellah Benzaouia** **

* *HTW Berlin, Department of Engineering I, Control Engineering, Berlin, Germany (e-mail: {schulte,soeren.georg}@ htw-berlin.de)*
** *LAEPT-URAC 28, University Cadi Ayyad, Faculty of Sciences Semlalia, Marrakech, Morocco, (e-mail: benzaouia@uca.ma)*

Abstract: In this paper, an observer bank design for sensor fault diagnosis and fault-tolerant control schemes for wind turbines with hydrostatic transmissions are presented. The sensor faults are detected and isolated by several observers using different sensor signals. Starting from a detailed problem formulation that takes into account structured model uncertainties and external inputs, the sufficient conditions for robust observer and controller design are obtained by using multiple Lyapunov functions. Thereafter, the drive train is modeled and the resulting nonlinear continuous-time system is transformed into a discrete-time Takagi-Sugeno form. Within the latter model, a fault-tolerant control scheme is set up by means of a switched observer-based parallel distributed controller (PDC) structure, where only the observed state vector, which is not affected by sensor faults, is fed back. Finally, the obtained results are applied to a fault tolerant speed control for wind turbines with hydrostatic transmission in the presence of permanent pressure or displacement sensor faults.

Keywords: Fault-Tolerant Control, Wind Turbines, Takagi-Sugeno Models, Observer Design

1. INTRODUCTION

Wind turbines with hydrostatic transmission are not yet available in commercial systems. Only recently, this drive-train concept has been considered as an alternative to conventional wind turbines. There are several reasons for this: Over the rated power range between 1.5 and 10 MW, the existing gearless direct-drive concepts cause an increase of weight around 25 percent and a cost increase of around 30 percent (Ragheb and Ragheb (2010)). The conventional gearboxes of modern wind turbines at the MegaWatt (MW) level of rated power are highly stressed by different load cases, where wind gusts and turbulence lead to misalignment of the drive train and a gradual failure of the gear components. This failure interval creates a significant increase in the capital and operating costs and downtime of a turbine, while greatly reducing its profitability and reliability (Ragheb and Ragheb (2010)). By contrast, the hydrostatic transmission allows mechanically decoupled operation over a wider range of wind speeds as a consequence of the omission of mechanical gearboxes and power converters. It permits the use of synchronous generators with low numbers of poles, which are cheaper than the induction generators and multi-pole synchron generators commonly used in variable speed machines today. According to the investigation in Diepeveen and Laguna (2011), hydrostatic transmissions also have a positive impact on power quality, since small rotor speed fluctuations due to wind gusts are absorbed.

Up to now, hydraulic transmissions are mainly used in construction and agricultural equipment. For these kind of applications, condition monitoring, fault diagnosis and maintenance are easy to perform. However, for a reliable operation of hydrostatic transmission in wind turbines, fault diagnosis and fault tolerant control are indispensable. Only a few model-based fault-tolerant control approaches exist for wind turbines with conventional drive-trains. In Sloth et al. (2011), passive and active fault-tolerant controllers are designed and considered with regard to accommodating altered actuator dynamics in the pitch system model. In Odgaard and Stoustrup (2012), a bank of unknown-input observers is used for fault diagnosis in the rotor and generator speed sensors of the FDI benchmark model presented in Odgaard et al. (2009). In Sami and Patton (2012b), fault-tolerant control is achieved in the partial-load region of wind turbines by means of a sensor fault hiding approach. The FTC strategy uses a multiple integral observer and a fast adaptive fuzzy estimator, where the observer designs are based on a nonlinear Takagi-Sugeno (TS) model. In Sami and Patton (2012a), a passive sensor fault-tolerant control strategy is implemented using a sliding mode controller for the partial-load region that tolerates generator speed sensor faults and generator torque offset faults. In Rotondo et al. (2013), an FTC strategy using Linear Parameter Varying (LPV) virtual sensors is proposed and applied to the benchmark model (Odgaard et al. (2009)). Instead of hiding the fault, the virtual sensor is used to expand the set of available sensors before the state observer is designed. In Georg and Schulte (2013), a Takagi-Sugeno sliding mode observer (TS SMO) is used to reconstruct actuator faults in wind turbines. Here, the proposed FTC strategy is based on the

modification of the control inputs with the reconstructed fault signals to achieve fault-tolerant control in the presence of actuator faults with a behaviour similar to the fault-free case.
In this paper, an observer bank design for sensor fault diagnosis and fault-tolerant control schemes for wind turbines with hydrostatic transmissions are presented. The sensor faults are detected and isolated by several observers using different sensor signals. The method takes into account both structured model uncertainties and external inputs. The fault-tolerant control scheme is set up by means of a switched observer-based parallel distributed controller (PDC) structure, where only the observed state vector, which is not affected by sensor faults, is used.
This paper is organized as follows: Section 2 deals with the problem formulation and preliminary results on fault detection and the FTC problem for switched Takagi-Sugeno models. Section 3 presents a mathematical model of a wind turbine drive train with a continuously variable hydrostatic transmission. The application of the fault tolerant control scheme and all design steps are presented in Section 4. First simulation results are discussed in Section 5.

2. PROBLEM FORMULATION

2.1 Discrete-time Takagi-Sugeno model with uncertainties

Consider the following discrete-time Takagi-Sugeno (TS) system:

$$\begin{aligned} \mathbf{x}(k+1) &= \mathbf{A_z}\mathbf{x}(k) + \Delta\mathbf{A_z}\,\mathbf{x}(k) + \mathbf{B_z}\mathbf{u}(k) + \mathbf{E_z}\mathbf{d}(k)\,, \\ \mathbf{y}(k) &= \mathbf{C_z}\,\mathbf{x}(k) + \mathbf{N_z}\,\mathbf{d}(k) + \mathbf{M_z}\,\mathbf{f}(k) \end{aligned} \tag{1}$$

where $k \in \mathbb{Z}_+$ is the dicrete-time, $\mathbf{x} \in \mathbb{R}^n$ is the state, $\mathbf{u} \in \mathbb{R}^m$ is the control input, $\mathbf{y} \in \mathbb{R}^p$ is the output, $\mathbf{d} \in \mathbb{R}^g$ is an external unknown input and $\mathbf{f} \in \mathbb{R}^q$ is the fault.
The matrices $\mathbf{A_z}, \Delta\mathbf{A_z}, \mathbf{B_z}, \mathbf{C_z}, \mathbf{E_z}, \mathbf{N_z}$ and $\mathbf{M_z}$ have the same following structure

$$\begin{aligned} \mathbf{A_z} &:= \sum_{i=1}^{N_r} h_i(\mathbf{z}(k))\mathbf{A}_i\,, \quad \Delta\mathbf{A_z} := \sum_{i=1}^{N_r} h_i(\mathbf{z}(k))\Delta\mathbf{A}_i\,, \\ \mathbf{B_z} &:= \sum_{i=1}^{N_r} h_i(\mathbf{z}(k))\mathbf{B}_i\,, \quad \mathbf{E_z} := \sum_{i=1}^{N_r} h_i(\mathbf{z}(k))\mathbf{E}_i\,, \\ \mathbf{C_z} &:= \sum_{i=1}^{N_r} h_i(\mathbf{z}(k))\mathbf{C}_i\,, \quad \mathbf{N_z} := \sum_{i=1}^{N_r} h_i(\mathbf{z}(k))\mathbf{N}_i\,, \\ \mathbf{M_z} &:= \sum_{i=1}^{N_r} h_i(\mathbf{z}(k))\mathbf{M}_i\,, \end{aligned} \tag{2}$$

where $\mathbf{A}_i, \mathbf{B}_i, \mathbf{C}_i, \mathbf{E}_i, \mathbf{N}_i$ and $\mathbf{M}_i$ are known real matrices of appropriate dimension and $\mathbf{z} \in \mathbb{R}^l$ is the scheduling vector. The TS membership functions $h_i \geq 0$ fulfill the convexity condition $\sum_{i=1}^{N_r} h_i(\mathbf{z}(k)) = 1 \;\; \forall \mathbf{z}$. Thus, the Takagi-Sugeno model (1) is a convex combination of linear submodels. This property facilitates the stability analysis for a class of nonlinear systems represented by (1). The weighted combination of unknown norm-bounded terms $\Delta\mathbf{A}_i$ takes into account parametric uncertainties in the system dynamics

$$\Delta\mathbf{A}_i = \mathbf{L}_i\;\mathbf{W}(k)\;\mathbf{H}_i\;, \tag{3}$$

where $\mathbf{L}_i$ and $\mathbf{H}_i$ are known real matrizes of appropriate size and $\mathbf{W}(k)$ is a unknown orthogonal matrix (function), which satisfies the condition

$$\mathbf{W}(k)^T\mathbf{W}(k) \leq \mathbf{I}\,, \tag{4}$$

with $\mathbf{I}$ as identity matrix Tanaka:2001. It is assumed that

- Each pair $(\mathbf{A}_i, \mathbf{C}_i^m)$ is observable, $i = 1, \ldots, N_r$, $m = 1, \ldots, p$, where $\mathbf{C}_i^m \in \mathbb{R}^{(p-1)\times n}$ stands for the matrix formed by all the rows of matrix $\mathbf{C}_i$ expect its m-th row.
- The matrices $\mathbf{C}_i$ are of full rank.
- At every discrete-time k, only one sensor is faulty

2.2 Extended state-space system for FTC design

To stabilize the TS system (1) a fault-tolerant observer-based state feedback is used. In this work we propose a bank of observers for the class of Takagi-Sugeno models The investigation is inspired by Benzaouia et al. (2012) but instead of using only switching functions an added extension with smooth nonlinear functions is introduced. For this, consider the following bank of $m = 1, \ldots, p$ observers:

$$\begin{aligned} \hat{\mathbf{x}}_m(k+1) = \sum_{i=1}^{N_r} h_i(\mathbf{z}(k))[&\mathbf{A}_i\,\hat{\mathbf{x}}_m(k) \\ &+ \mathbf{B}_i\,\mathbf{u} + \mathbf{K}_i^m(\mathbf{y}_m(k) - \hat{\mathbf{y}}(k)_m)]\,, \\ \hat{\mathbf{y}}_m(k) = \sum_{i=1}^{N_r} h_i(\mathbf{z}(k))\;&\mathbf{C}_i^m\,\hat{\mathbf{x}}_m(k)\,, \end{aligned} \tag{5}$$

where $\mathbf{x}_m(k)$ is the reconstructed vector without the faulty sensor of the m-th output and $\mathbf{y}_m$ stands for the vector formed by all the components of the vector $\mathbf{y}$ except its m-th component. Thus, the fault tolerant state reconstruction is based on a bank of observers with a maximum number of p individual observers, where $\mathbf{K}_i^m \in \mathbb{R}^{n\times(p-1)}$. $\hat{\mathbf{y}}_m, \mathbf{y}_m \in \mathbb{R}^{p-1}$. Note that

$$\mathbf{y}_m(k) = \sum_{i=1}^{N_r} h_i(\mathbf{z}(k))[\,\mathbf{C}_i^m\,\mathbf{x}_m(k) + \mathbf{N}_i^m\,\mathbf{d}(k) + \mathbf{M}_i^m\,\mathbf{f}(k)\,] \tag{6}$$

which will be used for the formal analysis of the observer error. To start with, the residuals of the observer bank are considered, which are defined as

$$\mathbf{r}_m = \sum_{i=1}^{N_r} \mathbf{V}_m(\mathbf{y}_m(k) - \hat{\mathbf{y}}_m(k))\,, \tag{7}$$

where the weighting matrices V_m are parameters to be designed. Defining the m-th observer error as

$$\mathbf{e}_m(k) = \mathbf{x}(k) - \hat{\mathbf{x}}_m(k) \tag{8}$$

leads to

$$\begin{aligned} \mathbf{e}_m(k+1) = \sum_{i=1}^{N_r}\sum_{j=1}^{N_r} &h_i(\mathbf{z}(k))\,h_j(\mathbf{z}(k))\big[\\ &(\mathbf{A}_i - \mathbf{K}_i^m\mathbf{C}_j^m)\,\mathbf{e}_m(k) + (\mathbf{E}_i - \mathbf{K}_i^m\mathbf{N}_j^m)\,\mathbf{d}(k) \\ &- \mathbf{K}_i^m\mathbf{M}_j^m\,\mathbf{f}(k) + \Delta\mathbf{A}_i(k)\,\mathbf{x}(k)\big]\,. \end{aligned} \tag{9}$$

In addition, to stabilize the system in the fault-free case, the controller has to achieve asymptotic stability in closed-

loop even in the presence of a single sensor fault. To achieve this, the following hybrid control law is introduced:

$$\mathbf{u}(k) = \sum_{i=1}^{N_r} \sum_{m=0}^{p} h_i(\mathbf{z}(k))\, \xi_m(J_m(k))\, \mathbf{F}_i^m\, \hat{\mathbf{x}}_m(k)\,, \qquad (10)$$

with h_i as the same smooth nonlinear functions as in the model (1) and switching functions ξ_m. The switching functions ξ_m depend on the residual criterion $J_m(k)$. Both will be defined in the next subsection. Note that the switching functions $\xi_m \in \{0,1\}$ satisfy the convex sum property $\sum_{i=1}^{N_r} \xi_m(J_m(k)) = 1$. Inserting (10) in (1) and after a short calculation, the closed loop system is obtained:

$$\begin{aligned}\mathbf{x}(k+1) = &\sum_{i=1}^{N_r}\sum_{j=1}^{N_r}\sum_{m=0}^{p} h_i(\mathbf{z}(k))\, h_j(\mathbf{z}(k))\, \xi_m(J_m(k)) \\ &\big[\, \big(\mathbf{A}_i + \mathbf{B}_i\, \mathbf{F}_j^m\big)\, \mathbf{x}(k) + \Delta\mathbf{A}_i \mathbf{x}(k) \\ &+ \mathbf{E}_i \mathbf{d}(k) - \mathbf{B}_i\, \mathbf{F}_j^m\, (\mathbf{x}(k) - \hat{\mathbf{x}}_m(k))\, \big]\,, \\ \mathbf{y}(k) = &\sum_{i=1}^{N_r} h_i(\mathbf{z}(k)) \big[\mathbf{C}_i \mathbf{x}(k) + \mathbf{N}_i\, \mathbf{d}(k) + \mathbf{M}_i\, \mathbf{f}(k)\big]\,. \end{aligned} \qquad (11)$$

Defining an augmented state vector as

$$\tilde{\mathbf{x}}(k) := [\, \mathbf{x}(k)^T\ \hat{\mathbf{x}}_m(k)^T\ \mathbf{e}_m(k)^T\,]^T$$

and an augmented input vector as

$$\mathbf{w}(k) := [\, \mathbf{d}(k)^T\ \mathbf{f}(k)^T\,]^T\,,$$

the corresponding dynamical system is derived as follows

$$\begin{aligned}\tilde{\mathbf{x}}_m(k+1) = &\sum_{i=1}^{N_r}\sum_{j=1}^{N_r}\sum_{m=0}^{p} h_i(\mathbf{z}(k))\, h_j(\mathbf{z}(k))\, \xi_m(J_m(k)) \\ &\big[\tilde{\mathbf{A}}_{c_i}^m\, \tilde{\mathbf{x}}_m(k) + \Delta\tilde{\mathbf{A}}_i\, \tilde{\mathbf{x}}_m(k) + \tilde{\mathbf{B}}_i^m\, \mathbf{w}(k)\big]\end{aligned} \qquad (12)$$

$$\mathbf{r}_m(k) = \sum_{i=1}^{N_r} h_i(\mathbf{z}(k)) \big[\mathbf{V}_m \left(\tilde{\mathbf{C}}_i^m\, \tilde{\mathbf{x}}_m(k) + \tilde{\mathbf{D}}_i^m\, \tilde{\mathbf{w}}(k)\right)\big] \qquad (13)$$

where

$$\tilde{\mathbf{A}}_{c_i}^m = \begin{bmatrix} \mathbf{A}_i + \mathbf{B}_i\, \mathbf{F}_j^m & 0 & -\mathbf{B}_i\, \mathbf{F}_j^m \\ 0 & \mathbf{A}_i + \mathbf{B}_i\, \mathbf{F}_j^m & \mathbf{K}_i^m \mathbf{C}_j^m \\ 0 & 0 & \mathbf{A}_i - \mathbf{K}_i^m \mathbf{C}_j^m \end{bmatrix},$$

$$\tilde{\mathbf{B}}_i^m = \begin{bmatrix} \mathbf{E}_i & 0 \\ -\mathbf{K}_i^m \mathbf{N}_j^m & -\mathbf{K}_i^m \mathbf{M}_j^m \\ \mathbf{E}_i - \mathbf{K}_i^m \mathbf{N}_j^m & -\mathbf{K}_i^m \mathbf{M}_j^m \end{bmatrix},$$

$$\Delta\tilde{\mathbf{A}}_i = \begin{bmatrix} \Delta\mathbf{A}_i(k) & 0 & 0 \\ 0 & 0 & 0 \\ \Delta\mathbf{A}_i(k) & 0 & 0 \end{bmatrix},$$

$$\tilde{\mathbf{C}}_i^m = \begin{bmatrix} 0 & 0 & \mathbf{V}_m \mathbf{C}_j^m \end{bmatrix}\,, \quad \tilde{\mathbf{D}}_i^m = \begin{bmatrix} \mathbf{V}_m \mathbf{N}_j^m & \mathbf{V}_m \mathbf{M}_j^m \end{bmatrix}\,.$$

The uncertain term for the augmented system can be again written as follows:

$$\Delta\tilde{\mathbf{A}}_i = \tilde{\mathbf{L}}_i\, \tilde{\mathbf{W}}\, \tilde{\mathbf{H}}_i\,, \qquad (14)$$

where

$$\tilde{\mathbf{L}}_i = \begin{bmatrix} \mathbf{L}_i & 0 & 0 \\ 0 & 0 & 0 \\ 0 & 0 & \mathbf{L}_i \end{bmatrix}, \quad \tilde{\mathbf{H}}_i = \begin{bmatrix} \mathbf{H}_i & 0 & 0 \\ 0 & 0 & 0 \\ 0 & 0 & \mathbf{H}_i \end{bmatrix},$$

and

$$\tilde{\mathbf{W}} = \mathrm{diag}\big(\mathbf{W}(k)\,,\, 0\,,\, \mathbf{W}(k)\big)\,.$$

2.3 Residual analysis and decision making

As mentioned in Benzaouia et al. (2012) a fault tolerant control scheme does not necessarily need the recontruction of faults. One can use the following residual criterion

$$J_m(k) = \begin{cases} \sum_{n=k}^{k_o+k} \sqrt{\mathbf{r}_m^T(n)\, \mathbf{r}_m(n)}\,, & k \leqslant T \\ \sum_{n=k-T}^{k} \sqrt{\mathbf{r}_m^T(n)\, \mathbf{r}_m(n)}\,, & k > T \end{cases} \qquad (15)$$

where $k_0 + k$ defines the interval of the moving average window, if the current sample time fulfills $k \leq T$. The size of the window increases until it is equal to the global fixed horizon of observation T. Then this criterion can be compared to a threshold J_{th} to decide whether a fault has occurred or not:

$$\begin{aligned} &\exists m \quad J_m(k) > J_{th}, \Rightarrow \text{Faults} \\ &\forall m \quad J_m(k) \leq J_{th}, \Rightarrow \text{No Faults} \end{aligned}$$

The threshold criterion can be chosen as indicated in Wang et al. (2009) as

$$\sup_{d \in l_2[0,\infty), \mathbf{f}=\mathbf{0}, k} J_0(k)\,, \qquad (16)$$

where $J_0(k)$ stands for a criterion obtained with a residual $\mathbf{r}_0$ computed with no sensor fault. Once the fault is detected, the problem is how to locate the faulty sensor. Note that one needs to compute the threshold criterion (16) and the 2-norm of all residuals $||\mathbf{r}_m||$. The faulty sensor noted by m_F can be located by the following method to check for $m = 1, \ldots, p$ at any time k:

$$\begin{aligned} &\text{IF } J_m(k) > J_{th} \text{ AND } ||\mathbf{r}_m|| > \min_{0 \leq m \leq p} ||\mathbf{r}_m|| \text{ THEN} \\ &\quad \text{Sensor } m \text{ is not faulty..} \\ &\text{IF } J_m(k) > J_{th} \text{ AND } ||\mathbf{r}_m|| > \min_{0 \leq m \leq p} ||\mathbf{r}_m|| \text{ THEN} \\ &\quad \text{Sensor } m_F = m \text{ is the faulty sensor..} \end{aligned} \qquad (17)$$

2.4 Stability conditions for FTC design

The following stability conditions are based on the cone complementarity technique introduced by Ghaoui et al. (1997) using LMI citeria with slack variables and multiple weighted residual matrices introduced by Nachidi et al. (2008), Gao and Chen (2008). A very common Lemma proposed by Shi et al. (1999) takes into account the model uncertainties (14):

Lemma 1. Given symmetric matrix $\mathbf{S}$ and matrices $\mathbf{L}$,$\mathbf{W}(k)$ and $\mathbf{H}$ of appropriate size, then

$$\mathbf{S} + \mathbf{L}^T\, \mathbf{W}(k)\, \mathbf{H}^T + \mathbf{H}^T\, \mathbf{W}^T(k)\, \mathbf{L} \leq \mathbf{0}$$

holds for $\mathbf{W}^T(k)\, \mathbf{W}^T(k) \leq \mathbf{I}$ if and only if there exists a scalar $\epsilon > 0$ such that

$$\mathbf{S} + \epsilon^{-1}\, \mathbf{L}^T\, \mathbf{L} + \epsilon\, \mathbf{H}^T\, \mathbf{H} \leq \mathbf{0}\,.$$

All results that are used here are described in detail in Benzaouia (2012) and Benzaouia et al. (2012). The sufficient criterion for the design formulated in LMI form is presented in the following Lemma:

Lemma 2. (Benzaouia (2012)) For a given scalar γ_m the system (12) is asymptotically stable for $\mathbf{w}(k) = \mathbf{0}$, $\tilde{\mathbf{x}}_0 \neq \mathbf{0}$ and with $\mathbf{w}(k) \neq \mathbf{0}$ under zero-initial conditions $\tilde{\mathbf{x}}_0 = \mathbf{0}$ if the performance index

$$\sup_{\mathbf{w}(k)\neq\mathbf{0},\mathbf{w}(k)\in l_2[0,\infty)} \frac{\sqrt{\mathbf{r}_m(k)^T\,\mathbf{r}_m(k)}}{\sqrt{\mathbf{w}_m(k)^T\,\mathbf{w}_m(k)}} < \gamma_m\,,\ \gamma_m > 0 \tag{18}$$

is guaranteed for all $\mathbf{w}(k) \in l_2[0,\infty)$, and if there exist positive definite symmetric matrices $\mathbf{P}_i^m$, $\mathbf{Q}_i^m$, $\mathbf{S}_i^m$, $\mathbf{R}_i^m$ and matrices $\mathbf{X}_i^m$, $\mathbf{Z}_i^m$, $\mathbf{K}_i^m$, $\mathbf{F}_i^m$, $\mathbf{V}^m$ for $i = 1,\ldots,N_r$, $m = 1,\ldots,p$ such that

$$\begin{bmatrix} -\mathbf{S}_i^m & \tilde{\mathbf{A}}_{c_i}^m & 0 & \tilde{\mathbf{B}}_i & 0 & 0 & \tilde{\mathbf{L}}_i^T \\ * & -\mathbf{\Gamma}_i^m & \mathbf{\Psi}_i & 0 & (\tilde{\mathbf{C}}_i^m)^T & \mathbf{I} & 0 \\ * & * & -\mathbf{\Lambda}_i^m & 0 & 0 & 0 & 0 \\ * & * & * & -\gamma_m^2\,\mathbf{I} & -(\tilde{\mathbf{D}}_i^m)^T & 0 & 0 \\ * & * & * & * & -\mathbf{I} & 0 & 0 \\ * & * & * & * & * & -\mathbf{R}_i^m & 0 \\ * & * & * & * & * & * & -\epsilon\,\mathbf{I} \end{bmatrix} < 0 \tag{19}$$

$$\begin{bmatrix} -\mathbf{X}_i^m - (\mathbf{X}_i^m)^T + \mathbf{P}_i^m & -\mathbf{X}_i^m - (\mathbf{X}_i^m)^T + \mathbf{I} \\ * & -\mathbf{X}_i^m - (\mathbf{X}_i^m)^T + \mathbf{S}_i^m \end{bmatrix} < 0 \tag{20}$$

$$\begin{bmatrix} -\mathbf{Z}_i^m - (\mathbf{Z}_i^m)^T + \mathbf{Q}_i^m & -\mathbf{Z}_i^m - (\mathbf{Z}_i^m)^T + \mathbf{I} \\ * & -\mathbf{Z}_i^m - (\mathbf{Z}_i^m)^T + \mathbf{R}_i^m \end{bmatrix} < 0 \tag{21}$$

where * stands for the symmetrical terms of the corresponding off-diagonal term.

3. CONTROL-ORIENTED MODELING

3.1 Drive train with hydrostatic transmission

In contrast to conventional drive trains, the inertia power in hydrostatic transmissions is transmitted by static pressure and flow rate. One advantage is that the gear ratio is continuously adjustable. In its simplest form, the hydrostatic transmission consists of a hydraulic pump and motor, of which at least one must have a variable displacement. A configuration with both a variable pump and a motor is illustrated in Figure 1. Another configuration with a fixed displacement pump and variable motor is investigated in Dolan and Aschemann (2012) for a gain scheduled linear quadratic regulator design.

On the transmission input side, the torque and speed of the rotor are converted by the hydraulic pump into a pressurised oil flow q_P. On the output side, the pressurised flow q_M is converted back into mechanical torque and speed by the hydraulic motor. By varying the displacement of the hydraulic components, any desired transmission ratio can be adjusted. This can be illustrated by the following considerations: The fluid flow q_P produced by the pump is proportional to its rotational speed ω_P and depends on the variable volume of the pump per revolution. Indeed, the volume is not constant and proportional to the normalised position of displacement unit

$$q_P = V_P\,\tilde{x}_P\,\omega_P \quad \text{with} \quad \tilde{x}_P = x_P/x_{P_{max}} \tag{22}$$

where V_P is the maximum volumetric displacement per revolution of the pump. Similarly, the volume flow through the hydraulic motor is given by

$$q_M = V_M\,\tilde{x}_M\,\omega_M \tag{23}$$

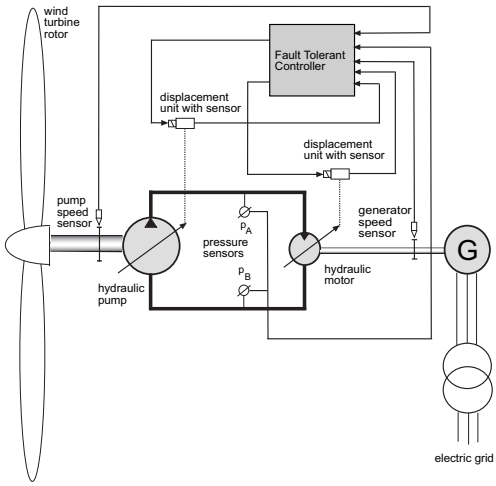

Fig. 1. Simplified hydrostatic drive train schematic

where $\tilde{x}_M$ denotes the normalised position of the displacement unit, and ω_M the rotational speed of the motor shaft. Figure 1 shows that the pump feeds directly the motor. Neglecting the compressibility of the fluid and hydrostatic losses it holds that $q_P = q_M$ and with (22), (23) we obtain

$$r = \frac{\omega_M}{\omega_P} = \frac{V_P}{V_M}\,\frac{\tilde{x}_P}{\tilde{x}_M}\,. \tag{24}$$

That is, the continously variable ratio r of the gear depends on the constant ratio of the maximum displacement of the pump/motor combination and the adjustable ratio of the position $\tilde{x}_P$ and $\tilde{x}_M$. The necessary high transmission ratio for wind turbines of the Megawatt class up to 2.5 MW can easily be reached by a suitably large ratio of the maximum displacements V_P/V_M. By taking advantage of the second adjustable term $\tilde{x}_P/\tilde{x}_M$, the transmission ratio can be varied in such a way that the generator operates at constant speed directly connected to the electric grid.

3.2 Reduced control-oriented model with uncertainties

The hydrostatic transmission dynamics can be represented by a fourth-order state-space model, proposed in Schulte and Gerland (2010). First, the actuator dynamics of the displacements units is taken into account by a first order lag element

$$\begin{aligned} \dot{\tilde{x}}_P &= -\frac{1}{\tau_{u_P}}\,\tilde{x}_P + \frac{k_P}{\tau_{u_P}}\,u_P\,, \\ \dot{\tilde{x}}_M &= -\frac{1}{\tau_{u_M}}\,\tilde{x}_M + \frac{k_M}{\tau_{u_M}}\,u_M \end{aligned} \tag{25}$$

with τ_{u_P} and τ_{u_M} as the time constants of the displacement units, k_P, k_M as static gains and u_P, u_M as the control signals. The pressure dynamics of the hydrostatic transmission in closed-circuit configuration can be modelled by

$$\Delta\dot{p} = \frac{10}{C_H}\,(V_P\,\tilde{x}_M\,\omega_P - V_M\,\tilde{x}_M\,\omega_M\ - k_{\text{leak}}\,\Delta p) \tag{26}$$

where Δp denotes the pressure difference in the closed-circuit, C_H denotes the hydraulic capacitance and k_{leak} denotes the leakage coefficient divided into a nominal value k_{leak_0} and an uncertainty Δk_{leak}

$$k_{\text{leak}} = k_{\text{leak}_0} + \Delta k_{leak}\,. \tag{27}$$

The dynamics of the drive train are governed by the equation of motion, which can be described by the following second order differential equation

$$\dot{\omega}_M = \frac{1}{J_{LSS}} \left(\eta_{mh} V_M \, 10^{-4} \, \tilde{x}_M \, \Delta p - d_{vc} \, \omega_M - T_g(\omega_g) \right) , \tag{28}$$

where J_{LSS} denotes the moment of inertia of the high speed rotor, η_{mh} denotes the hydromechanical efficiency, d_{vc} denotes the viscous damping coefficient and T_g is the electric torque of the generator as a function of the generator speed ω_g. Taking advantage of the continuously variable torque characteristics, a simple electrical configuration with a squirrel-cage induction generator (SCIG), directly coupled to the AC grid transformator (without power electronics), is studied, see Figure 1. The steady-state torque-speed characteristics of the SCIG, inspired by Bianchi et al. (2007), is given by

$$T_g(\omega_g) = -\frac{3}{2} \frac{U_s^2}{\omega_0} \frac{\frac{R_r}{s}}{(\frac{R_r}{s})^2 + (\omega_0 L_{lr})^2} , \quad s = \frac{\omega_0 - \omega_g}{\omega_0} , \tag{29}$$

where $\omega_s = 2\,\pi\, f_s$ denotes the angular line frequency, R_r and L_{lr} are the resistance and leakage inductance of the rotor windings, and s is the generator slip. In the slip equation (29), ω_0 denotes the synchronous speed of the induction generator. Note that the synchronous speed $\omega_0 = \frac{2}{p}\,\omega_s$ is imposed by the line frequency ω_s with p as the number of machine poles. Therefore, with a fixed voltage U_s and a fixed grid frequency $f_s = \omega_s/2\pi$, there is no active control on the generator. Finally, it is assumed that the flexibility of the drive shaft is negligible compared with the relatively low stiffness of the hydrostatic transmission. Thus, the identities are $\omega_P = \omega_r$ and $\omega_M = \omega_g$.

3.3 Discrete-time Takagi-Sugeno model

Starting from the nonlinear model equations (26),(25),(28) and the defined state vector $\mathbf{x} = [\,x_1\,,\,x_2\,,x_3\,,x_4\,]^T := [\,\tilde{x}_P\,,\,\tilde{x}_M\,,\Delta p\,,\omega_M\,]^T$ and input vector $\mathbf{u} = [\,u_1\,,\,u_2\,]^T := [\,u_P\,,\,u_M\,]^T$, an equivalent Takagi-Sugeno form is derived. Based on the proposed Takagi-Sugeno model of hydrostatic transmission in Schulte (2010), the extended structure is given by

$$\begin{aligned} \mathbf{x}(k+1) = &\sum_{i=1}^{N_r} h_i(\mathbf{z}(k)) \big((\mathbf{A}_i + \Delta\mathbf{A}_i)\,\mathbf{x}(k) \\ &+ \mathbf{B}_i\,\mathbf{u}(k) + \mathbf{E}_i\,\mathbf{d}(k) \big) \end{aligned} \tag{30}$$

$$\mathbf{y}(k) = \mathbf{C}\,\mathbf{x}(k) + \mathbf{N}\,\mathbf{d}(k) + \mathbf{M}\,\mathbf{f}(k) \; .$$

with $\mathbf{z}(k) := [\,\tilde{x}_M\,,\,\omega_r\,,\,\omega_g\,]^T$ as vector of scheduling variables. The extension refers to the additional variable ω_g in $\mathbf{z}(k)$, which increases the number of linear models from $N_r = 4$ to $N_r = 8$ submodels. Finally, the transformation from the continuous-time system (30) to discrete-time representation (1) is done in the usual way, whereby each submodel is separately transformed.

4. FAULT TOLERANT CONTROL SCHEME

The fault tolerant control scheme is illustrated in Figure 2. It is shown, that the measurement of the difference pressure and both positions of the displacement units are necessary for the control of the transmission ratio between the low and high speed shaft. For the observer bank (5) using (30) we define $m = 1, 2, 3$ output matrices:

$$\mathbf{C}^1 = \begin{bmatrix} 0 & 1 & 0 & 0 \\ 0 & 0 & 1 & 0 \end{bmatrix} , \; \mathbf{C}^2 = \begin{bmatrix} 1 & 0 & 0 & 0 \\ 0 & 0 & 1 & 0 \end{bmatrix} , \; \mathbf{C}^3 = \begin{bmatrix} 1 & 0 & 0 & 0 \\ 0 & 1 & 0 & 0 \end{bmatrix}$$

The decision making process in Figure 2 can be described as follows. Assume that at time k the sensor of the displacement unit of the pump is faulty ($\tilde{x}_P$):

(1) $m = 1$: The position sensor of the displacement unit of the hydro pump is omitted. In this case the input of the first observer are only $\mathbf{y}_1 = [\,\tilde{x}_M\,,\,\Delta p\,]^T$ and $\mathbf{u}$. Since the position sensor of the displacement unit of the pump is faulty, the corresponding residual will be lower than the threshold, which imply that the position sensor of the displacement unit of the pump is faulty.
(2) $m = 2$: The position sensor of the displacement unit of the hydro motor is omitted. In this case the input of the second observer are only $\mathbf{y}_2 = [\,\tilde{x}_P\,,\,\Delta p\,]^T$ and $\mathbf{u}$. Since the position sensor of the displacement unit of the pump is faulty, the corresponding residual will be greater as the threshold.
(3) $m = 3$: The pressure sensor of the closed hydraulic circuit is omitted. In this case the input of the third observer are only $\mathbf{y}_3 = [\,\tilde{x}_P\,,\,\tilde{x}_M\,]^T$ and $\mathbf{u}$. Since the position sensor of the displacement unit of the pump is faulty, the corresponding residual will be greater as the threshold.

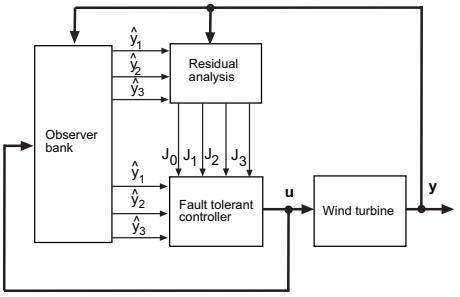

Fig. 2. Fault tolerant control scheme

5. SIMULATION

The simulation of the hydrostatic transmission in the error-free case is shown in Figure 3. In spite of the rotor speed variations due to wind speed fluctuations, the generator speed is kept approximately constant by the speed controller around the synchronous speed $\omega_0 = 2\,\pi\, f_s \left(\frac{2}{p}\right)$ for $p = 4$ and $f_s = 50\,\mathrm{Hz}$. The time variation of the normalised positions $\tilde{x}_P(t), \tilde{x}_M(t)$ of the displacement unit illustrate the operation of the hydrostatic transmission: The increasing displacement of the motor $V_M \cdot \tilde{x}_M(t)$ and the reduction of the pump displacement $V_P \cdot \tilde{x}_P(t)$ caused a decrease of the transmission ratio (24) in the time period $t = [3.5, 5.0]\,\mathrm{s}$ and vice versa in the time period $t = [6.5, 8.0]\,\mathrm{s}$. In Figure 4 a position sensor fault (offset error for $t \geq 6\,\mathrm{s}$) of the displacement unit of the hydro pump is illustrated by the fault diagnostic residuals and the fault tolerant control of the generator speed.

6. CONCLUSION AND CURRENT WORK

In this paper, an observer bank design on discrete-time Takagi-Sugeno systems with uncertainties are presented

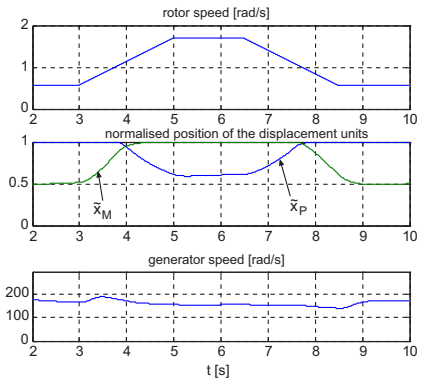

Fig. 3. Simulation results of the generator speed controller in the error free case

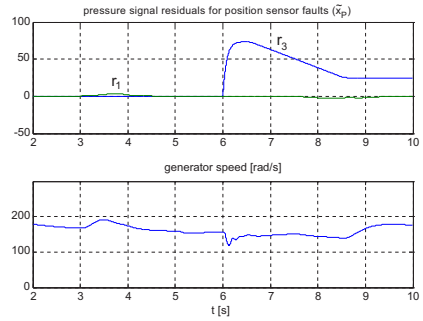

Fig. 4. Fault Diagnostic residuals and fault tolerant control of the generator speed

and applied to sensor fault isolation and fault-tolerant control for wind turbines with hydrostatic transmission. The current work consider a novel extension of the observer bank design with unmeasurable scheduling variables and study the influence of the residual analyis for robust decision making.

ACKNOWLEDGEMENTS

This research project is funded by the German Federal Ministry of Education and Research (BMBF) under grant no. 01DH13003.

REFERENCES

Benzaouia, A. (2012). *Saturated Switching Systems*. Springer-Verlag London-Limited.

Benzaouia, A., Ouladsine, M., and Ananou, B. (2012). Fault tolerant control of switching discrete-time systems with delay: an improved cone complementarity approach. *International Journal of System Science*, DOI: 10.1080/00207721.2012.762561, 1–11.

Bianchi, F.D., De Battista, H., and Mantz, R.J. (2007). *Wind Turbine Control Systems - Principles, Modelling and Gain Scheduling Design*. Springer-Verlag, London Limited.

Diepeveen, N. and Laguna, A. (2011). Dynamic modeling of fluid power transmissions for wind turbines. In *EWEA Offshore (The European Wind Energy Association)*. Amsterdam.

Dolan, B. and Aschemann, H. (2012). Control of a wind turbine with a hydrostatic transmission - an extended linearisation approach. In *17th International Conference on Methods and Models in Automation and Robotics (MMAR)*. Miedzyzdroje, Poland.

Gao, H. and Chen, T. (2008). Network-Based H_∞ Output Tracking Control. *IEEE Transactions on Automatic Control*, 53(3), 665–667.

Georg, S. and Schulte, H. (2013). Actuator Fault Diagnosis and Fault-Tolerant Control of Wind Turbines using a Takagi-Sugeno Sliding Mode Observer. In *International Conference on Control and Fault-Tolerant Systems (SysTol)*, 516–522. Nice, France.

Ghaoui, L.E., Oustry, F., and AitRami, M. (1997). A cone complementarity linearization algorithm for static output-feedback and related problem. *IEEE Transactions on Automatic Control*, 42(8), 1171–1176.

Nachidi, M., Benzaouia, A., and Tadeo, F. (2008). LMI Based Approach for Output-Feedback Stabilization for Discrete Time Takagi-Sugeno Systems. *IEEE Transactions on Fuzzy Systems*, 16(5), 1188–1196.

Odgaard, P.F. and Stoustrup, J. (2012). Fault Tolerant Control of Wind Turbines Using Unknown Input Observers. In *IFAC Symposium on Fault Detection, Supervision and Safety of Technical Processes*, 313–318. Mexico City, Mexico.

Odgaard, P.F., Stoustrup, J., and Kinnaert, M. (2009). Fault Tolerant Control of Wind Turbines - a benchmark model. In *IFAC Symposium on Fault Detection, Supervision and Safety of Technical Processes*, 155 – 160. Barcelona, Spain.

Ragheb, A.M. and Ragheb, M. (2010). Wind turbine gearbox technologies. In *1st International Nuclear & Renewable Energy Conference (INREC)*.

Rotondo, D., Puig, V., Valle, J.M.A., and Nejjari, F. (2013). FTC of LPV Systems using a Bank of Virtual Sensors: Application to Wind Turbines. In *International Conference on Control and Fault-Tolerant Systems (SysTol)*, 492–497. Nice, France.

Sami, M. and Patton, R.J. (2012a). Fault tolerant adaptive sliding mode controller for wind turbine power maximisation. In *7th IFAC Symposium on Robust Control Design*, 499–504. Aalborg, Denmark.

Sami, M. and Patton, R.J. (2012b). An FTC Approach to Wind Turbine Power Maximisation via T-S Fuzzy Modelling and Control. In *IFAC Symposium on Fault Detection, Supervision and Safety of Technical Processes*, 349–354. Mexico City, Mexico.

Schulte, H. (2010). LMI-based observer design on a power-split continuously variable transmission for off-road vehicles. In *Proceedings of IEEE Multi-conference on Systems and Control*. Yokohama, Japan.

Schulte, H. and Gerland, P. (2010). Observer-based estimation of pressure signals in hydrostatic transmissions. In *IFAC Symposium Advances in Automotive Control (AAC)*. Munich, Germany.

Shi, P., Boukas, E., and Agarwal, C. (1999). Control of markovian jump discrete-time systems with norm bounded uncertainty and unknown delay. *IEEE Transactions on Automatic Control*, 44(11), 2139–2144.

Sloth, C., Esbensen, T., and Stoustrup, J. (2011). Robust and fault-tolerant linear parameter-varying control of wind turbines. *Mechatronics*, 21, 645–659.

Wang, D., Wang, W., and Shi, P. (2009). Robust fault detection for switched systems with state delays. *IEEE Trans. on Systems and Cybernetics-B*, 39, 800–805.